Inorganic Chemistry

Article

pubs.acs.org/IC

Filling Gaps in the Series of Noninnocent Hetero-1,3-diene Chelate Ligands: Ruthenium Complexes of Redox-Active α-Azocarbonyl and α-Azothiocarbonyl Ligands RNNC(R′)E, E = O or S

Fabian Ehret,[†] Martina Bubrin,[†] Ralph Hübner,[†] David Schweinfurth,[†] Ingo Hartenbach,[†] Stanislav Záliš,[‡] and Wolfgang Kaim*[,†]

[†]Institut für Anorganische Chemie, Universität Stuttgart, Pfaffenwaldring 55, D-70569 Stuttgart, Germany

[‡]J. Heyrovský Institute of Physical Chemistry, v.v.i., Academy of Sciences of the Czech Republic, Dolejškova 3, CZ-18223 Prague, Czech Republic

Supporting Information

ABSTRACT: The series of 4-center unsaturated chelate ligands A═B−C═D with redox activity to yield $^{-}$A−B═C−D^{-} in two steps has been complemented by two new combinations RNNC(R′)E, E = O or S, R = R′ = Ph. The ligands *N*-benzoyl-*N*′-phenyldiazene = L_O, and *N*-thiobenzoyl-*N*′-phenyldiazene = L_S, (obtained in situ) form structurally characterized compounds $[(acac)_2Ru(L)]$, **1** with L = L_O, and **3** with L = L_S, and $[(bpy)_2Ru(L)](PF_6)$, **2**(PF_6) with L = L_O, and **4**(PF_6) with L = L_S ($acac^-$ = 2,4-pentanedionato; bpy = 2,2′-bipyridine). According to spectroscopy and the N−N distances around 1.35 Å and N−C bond lengths of about 1.33 Å, all complexes involve the monoanionic (radical) ligand form. For **1** and **3**, the antiferromagnetic spin−spin coupling with electron transfer-generated Ru^{III} leads to diamagnetic ground states of the neutral complexes, whereas the cations $\mathbf{2}^+$ and $\mathbf{4}^+$ are EPR-active radical ligand complexes of Ru^{II}. The complexes are reduced and oxidized in reversible one-electron steps. Electron paramagnetic resonance (EPR) and UV−vis−NIR spectroelectrochemistry in conjunction with time-dependent density functional theory (TD-DFT) calculations allowed us to assign the electronic transitions in the redox series, revealing mostly ligand-centered electron transfer: $[(acac)_2Ru^{III}(L^0)]^+ \rightleftharpoons [(acac)_2Ru^{III}(L^{\bullet-})] \rightleftharpoons [(acac)_2Ru^{III}(L^{2-})]^-/[(acac)_2Ru^{II}(L^{\bullet-})]^-$, and $[(bpy)_2Ru^{III}(L^{\bullet-})]^{2+}/[(bpy)_2Ru^{II}(L^0)]^{2+} \rightleftharpoons [(bpy)_2Ru^{II}(L^{\bullet-})]^+ \rightleftharpoons [(bpy)_2Ru^{II}(L^{2-})]^0$. The differences between the O and S containing compounds are rather small in comparison to the effects of the ancillary ligands, $acac^-$ versus bpy.

INTRODUCTION

Among the most widely used redox-active ligands[1] in coordination chemistry are the four-center hetero-1,3-diene chelate systems (Scheme 1) which can undergo stepwise reversible one-electron uptake, involving a radical ion intermediate.

Scheme 1

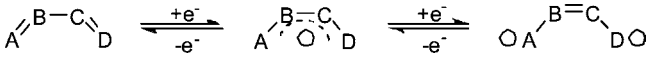

The noninnocent behavior[2] of ligands in complexes with redox-active transition metals can be analyzed via structure analysis because of mostly reliable bond order/bond length correlations.[3] Scheme 2 summarizes combinations of which several are well established;[4−13] one α-azocarbonyl example[14] has been observed earlier during attempts to prepare dinuclear compounds.

Electron affinity studies[15] have shown comparable electron acceptor properties of the azo and the thiocarbonyl function, the latter being a better π acceptor than the carbonyl group.[16] The *N*-thiobenzoyl-*N*′-phenyldiazene L_S is not stable in free form but can be generated in situ from bis[α-(phenylhydrazono)-phenyl]disulfide.[17] This precursor has now been crystallized and its structure determined (see Supporting Information).

Herein we describe the use of α-azocarbonyl and α-azothiocarbonyl "hybrid" hetero-1,3-diene ligands (Scheme 3) in connection with two ruthenium complex fragments, namely, the electron-rich $[Ru(acac)_2]$[15] and the more electron-deficient $[Ru(bpy)_2]^{2+}$.

Structural studies revealed the identities of the isolated ruthenium complexes, and cyclic voltammetry in combination with spectroelectrochemistry (UV−vis−NIR, EPR) provided information on the nature of the accessible redox states.

EXPERIMENTAL SECTION

Compound 1. A 250 mg portion (0.66 mmol) of $Ru(acac)_2(MeCN)_2$[19a] and 139 mg (0.66 mmol) of *N*-benzoyl-*N*′-phenyldiazene[20] were dissolved in CH_2Cl_2/toluene (5: 1) and stirred at 45 °C for 12 h under argon. The solvent was removed, and the red solid purified by column chromatography (aluminum oxide, CH_2Cl_2/MeCN 200: 1). Yield: 213 mg (63%). Anal. Calcd. for $C_{23}H_{24}N_2O_5Ru$ (509.52 g/mol): C, 54.22; H, 4.75; N, 5.50. Found: C, 54.15; H, 4.65; N, 5.14. ^{1}H NMR (250 MHz, CD_2Cl_2): δ[ppm] = 1.98 (s, 3H, acac), 2.10 (s, 3H, acac), 2.18 (s, 3H, acac), 2.43 (s, 3H, acac), 5.21 (s, 1H, acac), 5.66 (s, 1H, acac), 7.30−7.38 (m, 2H, Ph), 7.47−7.60 (m, 3H, Ph),

Received: February 29, 2012
Published: May 17, 2012

   dx.doi.org/10.1021/ic300439h | *Inorg. Chem.* 2012, 51, 6237−6244

Scheme 2

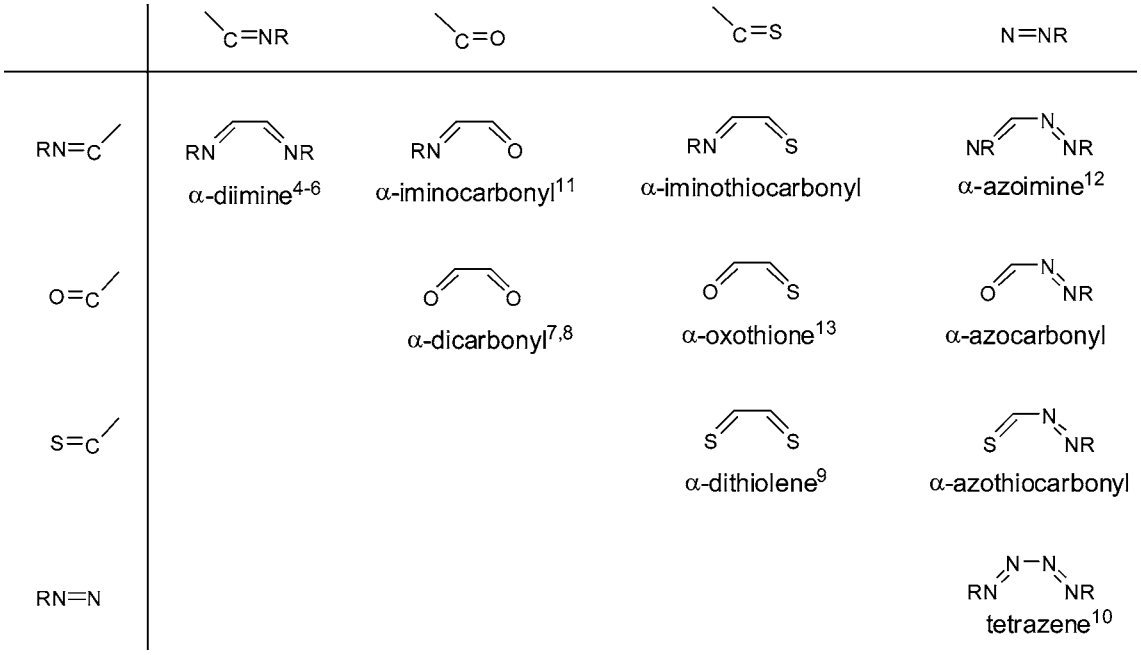

Scheme 3

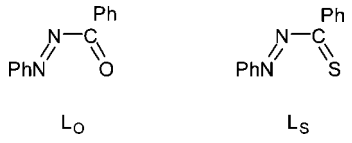

7.75–7.83 (m, 1H, Ph), 8.30–8.38 (m, 2H, Ph), 8.43–8.64 (m, 2H, Ph). ESI-MS Calcd (found) for **1**: *m*/*z* 510.07 (510.08).

Compound 2(PF_6). A 200 mg portion (0.38 mmol) of $Ru(bpy)_2Cl_2{\cdot}2H_2O$[19b] and 214 mg (0.85 mmol) of $AgPF_6$ were dissolved in acetone and refluxed for 2 h. The precipitate of AgCl was filtered through Celite. To the red solution were added 81 mg (0.38 mmol) of *N*-benzoyl-*N*′-phenyldiazene,[20] and the mixture was stirred at 60 °C for 12 h under argon. After evaporation of the solvent the crude product was purified by column chromatography (aluminum oxide, CH_2Cl_2/MeCN 8: 2) to give a green solid. Yield 239 mg (81%). Anal. Calcd. for $C_{33}H_{26}F_6N_6OPRu$ (623.67 g/mol)·$0.1CH_2Cl_2$: C, 51.57; H, 3.41; N, 10.93. Found: C, 51.16; H, 3.40; N, 10.81. ESI-MS Calcd (found) for $\mathbf{2}^+$: *m*/*z* 624.12 (624.12).

Compound 3. A 250 mg portion (0.66 mmol) of $Ru(acac)_2(MeCN)_2$[19a] and 300 mg (0.66 mmol) bis[α-(phenylhydrazono)-phenyl]disulfide[21] (**5**) were dissolved in CH_2Cl_2/toluene (5: 1) and stirred at 45 °C for 12 h under argon. The solvent was removed, and the red-violet solid purified by column chromatography (silica, CH_2Cl_2/MeCN 10: 1). Yield: 212 mg (61%). Anal. Calcd. for $C_{23}H_{24}N_2O_4RuS$ (525.58 g/mol): C, 52.56; H, 4.60; N, 5.33. Found: C, 52.48; H, 4.59; N, 5.32. ^{1}H NMR (250 MHz, acetone-d_6): δ [ppm] = 1.79 (s, 3H, acac), 1.84 (s, 3H, acac), 1.97 (s, 3H, acac), 2.33 (s, 3H, acac), 5.19 (s, 1H, acac), 5.70 (s, 1H, acac), 7.36–7.43 (m, 2H, Ph), 7.56–7.67 (m, 4H, Ph), 7.95–7.99 (m, 2H, Ph), 8.48–8.49 (m, 2H, Ph). ESI-MS Calcd (found) for **3**: *m*/*z* 526.05(526.06).

Compound 4(BF_4). A 200 mg portion (0.38 mmol) of $Ru(bpy)_2Cl_2{\cdot}2H_2O$[19b] and 165 mg (0.85 mmol) of $AgBF_4$ were dissolved in acetone and refluxed for 2 h. The precipitate of AgCl was filtered through Celite. To the red solution were added 173 mg (0.38 mmol) of bis[α-(phenylhydrazono)phenyl]disulfide[21] (**5**), and the mixture was stirred at 60 °C for 12 h under argon. After evaporation of the solvent, the crude product was purified by column chromatography (aluminum oxide, CH_2Cl_2/MeCN 8: 2) to give a green solid. Yield 226 mg (78%). Anal. Calcd. for $C_{33}H_{26}BF_4N_6SRu$ (726.54 g/mol): C, 54.55; H, 3.61; N, 11.57. Found: C, 54.11; H, 3.26; N, 11.38. ESI-MS Calcd (found) for $\mathbf{4}^+$: *m*/*z* 640.10 (640.10). **4**(PF_6) was prepared under the same conditions as **4**(BF_4), using $AgPF_6$. Yield 227 mg (76%). Anal. Calcd. for $C_{33}H_{26}F_6N_6PRuS$ (784.70 g/mol): C, 50.51; H, 3.34; N, 10.71. Found: C, 50.73; H, 3.39; N, 10.53.

Instrumentation. Electron paramagnetic resonance (EPR) spectra in the X band were recorded with a Bruker System EMX. ^{1}H NMR spectra were taken on a Bruker AC 250 spectrometer. IR spectra were obtained using a Nicolet 6700 FT-IR instrument; solid state IR measurements were performed with an ATR unit (smart orbit with diamond crystal). UV–vis–NIR absorption spectra were recorded on J&M TIDAS and Shimadzu UV 3101 PC spectrophotometers. A Bruker Micro TOF Q instrument was used to record the ESI-MS spectra (CH_3OH as solvent). Cyclic voltammetry was carried out in 0.1 M Bu_4NPF_6 solutions using a three-electrode configuration (Pt working and counter electrodes, Ag reference) and a PAR 273

Scheme 4

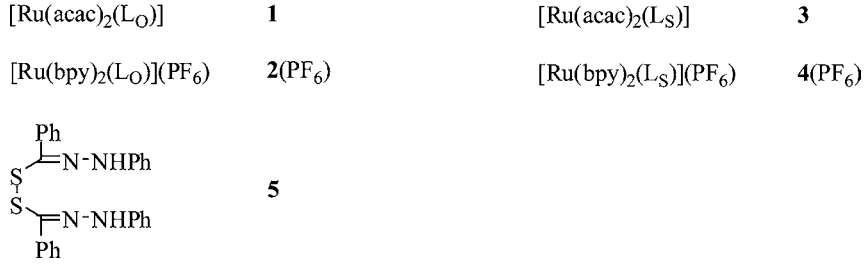

dx.doi.org/10.1021/ic300439h | Inorg. Chem. 2012, 51, 6237–6244

Table 1. Selected Crystallographic Data

	1	2(PF_6)	3	4(PF_6)	5
mol formula	$C_{23}H_{24}N_2O_5Ru$	$C_{33}H_{26}F_6N_6OPRu$	$C_{23}H_{24}N_2O_4RuS$	$C_{33}H_{26}F_6N_6PRuS$	$C_{26}H_{22}N_4S_2$
Fw	510.07	768.64	525.57	784.70	454.60
temp (K)	100(2)	100(2)	100(2)	100(2)	298(2)
cryst sym	triclinic	monoclinic	monoclinic	monoclinic	monoclinic
space group	$P\bar{1}$	$P2_1/c$	$P2_1/c$	$P2_1/c$	$P2_1/c$
a (Å)	8.7692(4)	12.9570(6)	16.4704(5)	10.570(2)	17.5049(7)
b (Å)	12.2019(8)	16.4648(7)	14.3426(5)	8.820(2)	7.9089(3)
c (Å)	12.53354(9)	16.8146(7)	9.4783(3)	33.470(6)	17.6023(7)
α (deg)	70.921(3)	90.00	90.00	90.00	90.00
β (deg)	70.309(3)	101.689(2)	97.306(1)	98.853(4)	106.705(2)
γ (deg)	74.557(3)	90.00	90.00	90.00	90.00
V (Å^3)	1174.8(4)	3512.7(3)	2220.8(1)	3083.4(9)	2334.10
Z	2	4	4	4	4
μ (mm^{-1})	0.709	0.559	0.832	0.701	0.249
D_{calcd} (g cm^{-3})	1.531	1.453	1.572	1.690	1.294
F (000)	556	1548	1072	1580	952
2θ range (deg)	2.84 to 27.12	1.60 to 30.57	2.50 to 30.50	1.95 to 25.22	2.37 to 25.15
data/restraints/parameters	5140/0/303	10714/0/478	6771/0/285	4455/0/460	4128/0/290
R_1, wR2 (all data)	0.1247, 0.1356	0.0400, 0.0797	0.0262, 0.0602	0.1160, 0.1378	0.0691, 0.1488
R_1, wR2 [$I > 2\sigma(I)$]	0.0710, 0.1165	0.0301, 0.0760	0.0230, 0.0586	0.0626, 0.1106	0.0510, 0.1416
GOF	1.096	1.056	1.045	1.134	1.041
largest diff. peak/hole (e Å^{-3})	0.707 and −0.788	0.602 and −0.560	0.652 and −0.652	0.865 and −0.865	0.198 and −0.237

potentiostat and function generator. The ferrocene/ferrocenium (Fc/Fc^+) couple served as internal reference. Spectroelectrochemistry was performed using an optically transparent thin-layer electrode (OTTLE) cell.[18a] A two-electrode capillary served to generate intermediates for X band EPR studies.[18b]

Crystallography. Crystallization procedures were as follows. Complex **1**: slow evaporation of a solution of **1** in MeOH/toluene at 4 °C; **2**(PF_6): slow diffusion of Et_2O into a solution of **2**(PF_6) in MeCN at 4 °C; **3**: slow evaporation of a solution of **3** in *n*-pentane at −20 °C; **4**(PF_6): slow diffusion of Et_2O into a solution of **4**(PF_6) in MeCN at 4 °C. X-ray diffraction (XRD) data were collected using a Bruker Kappa Apex2duo diffractometer. The structures were solved and refined by full-matrix least-squares techniques on F^2 using the SHELX-97 program.[22a] The absorption corrections were done by the multiscan technique. The PF_6 anions were found disordered. Since the solvent molecules could not be located in **2**(PF_6), the PLATON/SQEEZE procedure[22b] was used. All data were corrected for Lorentz and polarization effects, and the non-hydrogen atoms were refined anisotropically. Hydrogen atoms were included in the refinement process as per the riding model.

DFT Calculations. The electronic structures of the complexes **1**^{n}, **3**^{n} (n = −1, 0, 1) and **2**^{m}, **4**^{m} (m = 0, 1, 2) were calculated by density functional theory (DFT) methods using the Gaussian 09[23] and ADF2010.01[24,25] program packages. For the H, C, N, O, and S atoms 6-31G* polarized double-ζ basis sets[26] (G09) were used together with quasirelativistic effective core pseudopotentials and a corresponding optimized set of basis functions for Ru.[27] All structures were optimized without geometrical constraints using the hybrid PBE0 functional,[28,29] and open shell systems were treated within the UKS approach. Vibrational analysis was done to characterize minima. Electronic excitations were calculated by the time-dependent density functional theory (TD-DFT) method. The polarizable continuum model[30] (PCM) was used for modeling the solvent influence.

Slater type orbital (STO) basis sets of quadruple-ζ quality with four polarization functions for the Ru atoms and of triple-ζ quality with two polarization functions for the remaining atoms were employed within ADF2010.01. The inner shells were included in the calculations. The calculations of the g tensors were done with the functional including Becke's gradient correction[31] to the local exchange expression in conjunction with Perdew's gradient correction[32] to the local correlation (ADF/BP). The scalar relativistic zero order regular approximation (ZORA) was used within the ADF calculations. The g tensor was obtained from a spin-nonpolarized wave function after incorporating spin−orbit coupling. g and A tensors (PBE0 functional) were obtained by first-order perturbation theory from a ZORA Hamiltonian in the presence of a time-independent magnetic field.[33]

RESULTS AND DISCUSSION

In contrast to *N*-benzoyl-*N*′-phenyldiazene,[20] L_O, the *N*-thiobenzoyl-*N*′-phenyldiazene L_S is not stable in free form.[17a] However, it can be generated in situ by various reactions from the precursor

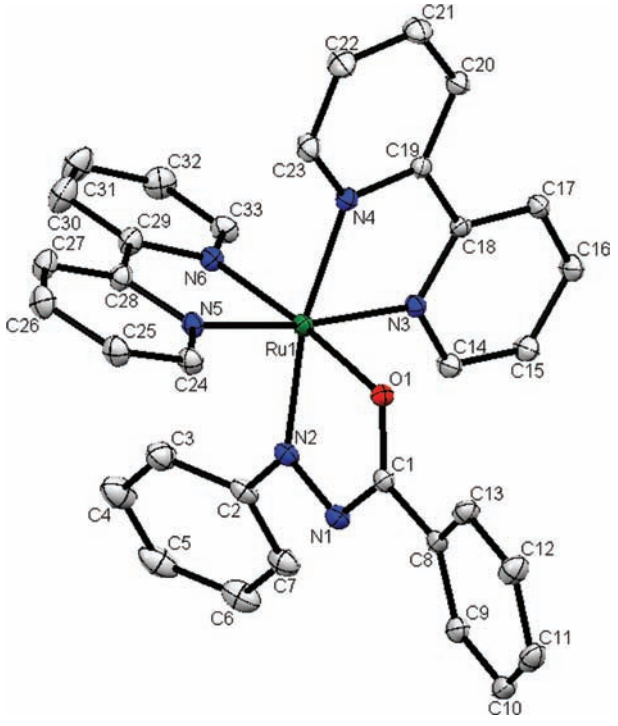

Figure 1. Molecular structure of the cation in the crystal of **2**(PF_6).

dx.doi.org/10.1021/ic300439h | Inorg. Chem. 2012, 51, 6237−6244

bis[α-(phenylhydrazono)phenyl]disulfide, **5** (Scheme 4).[17,21] Compound **5** has now been crystallized, and its structure determined (see Table 1 and Supporting Information); the S−S bonds at 2.068(1) Å and the N−N bonds at 1.329(3) and 1.331(3) Å support the formulation of **5** (Supporting Information, Table S1, Figure S1).

The reactions of the precursors $Ru(acac)_2(CH_3CN)_2$ and $Ru(bpy)Cl_2{\cdot}2H_2O$ with L_O or **5** proceeded to yield the complexes **1**, **2**(PF_6), **3**, and **4**(PF_6) (Scheme 4). As will be shown below, all complexes contain the monoanionic forms of the ligands, $L_O^{\bullet-}$ and $L_S^{\bullet-}$, and the convergence to these forms with internal (1) or external electron transfer under participation of the environment is in agreement with the electrochemical potential situation (see Table 3).

$$Ru^{II}(acac)_2(CH_3CN)_2 + L_O^{\circ} \rightarrow [Ru^{III}(acac)_2(L_O^{\bullet-})](\mathbf{1}) + 2CH_3CN \quad (1)$$

Molecular Structures. The complexes from Scheme 4 could be crystallized for X-ray structure analysis (Table 1). Two representative examples are shown in Figures 1 and 2, the bond lengths within the five-membered chelate rings are summarized in Table 2.

The data reveal rather invariant N−N and N−C distances of 1.35 Å and 1.33 Å, respectively, signifying bond orders of about 1.5[34] in accordance with a monoanion formulation [RNNC(R′)E]$^-$ in each case. Slight variations can be interpreted in terms of more pronounced reduction for the cations $\mathbf{2}^+$ and $\mathbf{4}^+$ (smallest N−C, long N−N distances) in comparison to the neutral **1** and **3**. The Ru−N distances (Table 2) illustrate stronger bonds in **1** and **3** relative to $\mathbf{2}^+$ and $\mathbf{4}^+$. The Ru−O and Ru−S bond lengths exhibit a less pronounced differentiation but are not unusual, the C−O and C−S distances reflect the fractional bond orders between 1 and 2.[35]

The neutral complexes **1** and **3** exhibit conventional NMR signals. Considering the structural evidence for monoanionic ligand states and the overall neutrality we infer a strong antiferromagnetic spin-pairing interaction between the one-electron reduced ligands, $L^{\bullet-}$, and the one-electron oxidized metal, Ru^{III}, which are formed in an electron transfer involving reaction 1. The diamagnetic species **1** and **3** are EPR silent. The alternative between (i) antiferromagnetically coupled ligand radical anion coordinated to an oxidized metal versus (ii) strong back-bonding between the nonoxidized metal and the unreduced acceptor is a classical one, going back to Weiss's and Pauling's different descriptions of metal−ligand bonding in

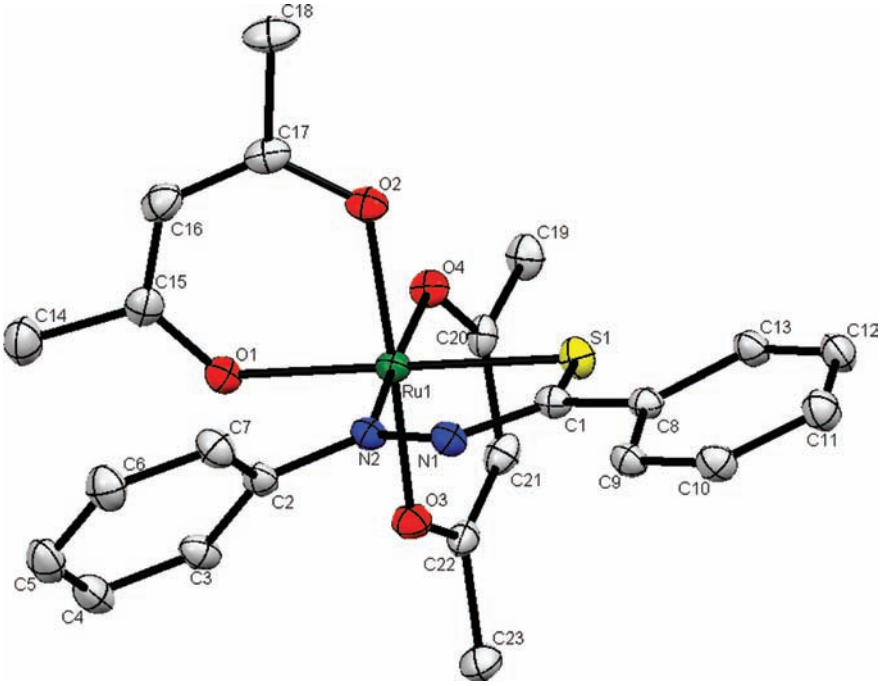

Figure 2. Molecular structure of **3** in the crystal.

Table 2. Representative Experimental and DFT Calculated Bond Lengths (Å) in the Ru−N−N-C-E Chelate Rings of 1, 2(PF_6), 3, and 4(PF_6)

	1		**2**(PF_6)		**3**		**4**(PF_6)	
bond	exp.	calc.	exp.	calc.	exp.	calc.	exp.	calc.
Ru−N2	1.902(5)	1.882	2.018(1)	2.055	1.931(1)	1.906	2.010(6)	2.044
Ru−O2	2.029(4)	2.020	2.051(2)	2.030				
Ru−S					2.2558(4)	2.274	2.318(2)	2.328
N1−N2	1.355(7)	1.325	1.367(2)	1.336	1.333(1)	1.318	1.355(7)	1.321
N1−C1	1.338(8)	1.344	1.322(2)	1.325	1.344(1)	1.331	1.318(9)	1.320
C1−O1	1.287(7)	1.268	1.297(2)	1.286				
C1−S					1.696(1)	1.699	1.727(8)	1.726

dx.doi.org/10.1021/ic300439h | Inorg. Chem. 2012, 51, 6237−6244

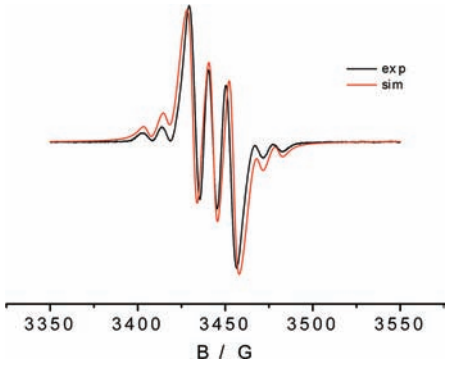

Figure 3. EPR spectrum of **2**(PF_6) in CH_2Cl_2 at 298 K (experimental and simulated with the data from Table 3).

Table 3. EPR Data for 1−4 in Various Oxidation States from Electrochemical Generation in CH_2Cl_2/0.1 M NBu_4PF_6

	1^-	1^+	2^+	3^-	4^+
g^a	2.035	n.o.	2.007	2.025	2.011
$g_1{}^b$	2.085	2.220	*c*	2.092	*c*
$g_2{}^b$	2.045	2.097	*c*	2.034	*c*
$g_3{}^b$	1.966	1.934	*c*	1.930	*c*
$g_1 - g_3$	0.119	0.286	<0.05	0.162	<0.05
$g_{iso}{}^d$	2.032	2.087		2.020	
$A(^{14}N)^e$	n.o.	n.o.	10.0	n.o.	8.5
$A(^{99,101}Ru)^e$	n.o.	n.o.	10.0	n.o.	13.8

[a]298 K. [b]110 K. [c]Unresolved *g* anisotropy. [d]Calculated from $g_{iso} = ((g_1^2 + g_2^2 + g_3^2)/3)^{1/2}$. [e]Coupling constants *A* in Gauss from 298 K spectra. The spectrum of 3^+ could not be analyzed.

Table 4. DFT Calculated EPR Data for 1−4 in Various Oxidation States

	1^-	1^+	2^+	3^-	3^+	4^+
g_1	2.073	2.164	2.028	2.092	2.138	2.038
g_2	1.993	2.065	2.006	2.034	2.077	2.002
g_3	1.952	1.938	1.996	1.930	1.969	1.985
$g_1 - g_3$	0.121	0.226	0.032	0.162	0.169	0.053
$g_{iso}{}^a$	2.007	2.056	2.010	2.020	2.061	2.009
$A(^{14}N)^b$			9.38			8.5
$A(^{99,101}Ru)^b$			7.10			13.8
Ru spin density	0.476	0.742	0.088	0.498		0.141

[a]Calculated from $g_{iso} = ((g_1^2 + g_2^2 + g_3^2)/3)^{1/2}$. [b]Coupling constants *A* in Gauss.

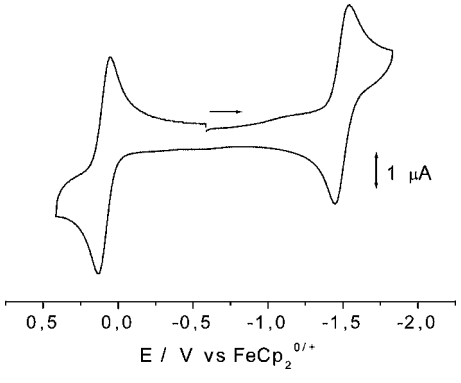

Figure 4. Cyclic voltammogram of **1** in CH_2Cl_2/0.1 M Bu_4NF_6 (100 mV/s scan rate).

Table 5. Redox Potentials[a,b] and Comproportionation Constants (K_c)[c] for 1, 2(PF_6), 3, and 4(PF_6)

compound	$E°_{298}$/V	(ΔE/V)		K_c
1	0.12	−1.48	(1.60)	1.3×10^{27}
2(PF_6)	−0.21	−1.23	(1.02)	3.0×10^{17}
3	0.48	−1.07	(1.55)	1.9×10^{26}
4(PF_6)	−0.14	−0.87	(0.73)	2.4×10^{12}

[a]Potentials $E°_{298}$/V versus $Fc^{0/+}$. [b]In CH_2Cl_2/0.1 M Et_4NPF_6/scan rate 100 mV s^{-1}. [c]$RT \ln K_c = nF(\Delta E)$.

Scheme 5

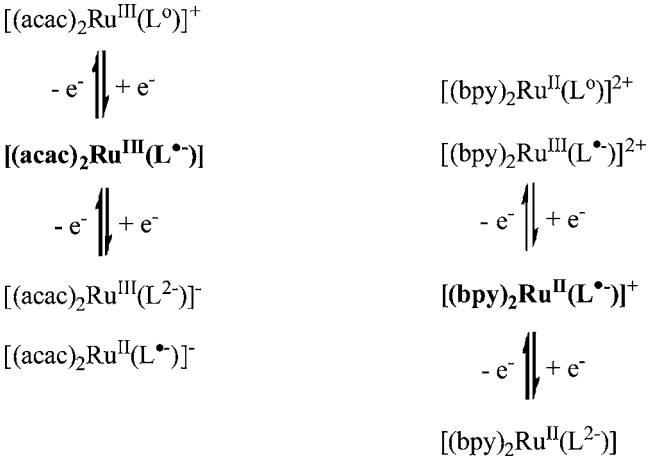

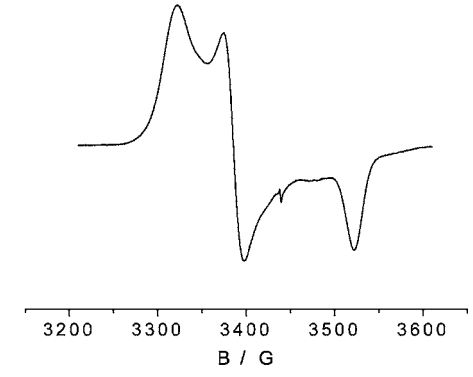

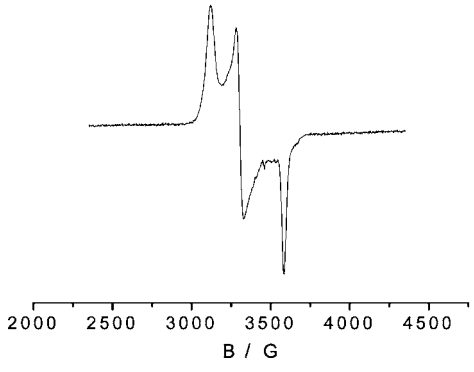

Figure 5. EPR spectra of 1^- (top) and 1^+ (bottom) in CH_2Cl_2/0.1 M Bu_4NPF_6 at 110 K.

dx.doi.org/10.1021/ic300439h | *Inorg. Chem.* 2012, 51, 6237−6244

oxy-myoglobin, namely, Fe^{III}-($O_2^{\bullet-}$) versus Fe^{II}-(O_2).[36] For the structural reasons given (short Ru–N, intermediate N–N distances, supported by DFT), we prefer alternative (i).

The EPR analysis of paramagnetic $\mathbf{2}^+$ and $\mathbf{4}^+$ in CH_2Cl_2 solution at room temperature yields well resolved spectra near g = 2, with hyperfine coupling from ^{14}N and $^{99,101}Ru$ isotopes (^{99}Ru, I = 5/2, 12.7% nat. abundance, A_{iso} = −62.94 mT; ^{101}Ru; I = 5/2, 17.0% nat. abundance, A_{iso} = −70.52 mT) (Figure 3, Table 3).

The ^{14}N and $^{99,101}Ru$ coupling constants (Table 3) indicate a ruthenium(II) complex of a semiquinone-type radical ligand.[18b,37] The higher g for $\mathbf{4}^+$ versus $\mathbf{2}^+$ reflects the spin–orbit coupling contribution from the sulfur atom, and the smaller ^{14}N but higher $^{99,101}Ru$ coupling of $\mathbf{4}^+$ suggests a slightly higher metal versus ligand contribution to the singly occupied molecular orbital (SOMO) in the S system. The DFT approach (Table 4) confirms the experimental results and their interpretation.

Spin densities of $\mathbf{1}^-$, $\mathbf{1}^+$, and $\mathbf{2}^+$ are depicted and compared in Supporting Information, Figure S2; the plots of spin densities of $\mathbf{3}^-$, $\mathbf{3}^+$, and $\mathbf{4}^+$ have similar shapes.

All four isolated complexes undergo each one reversible oxidation and one reversible reduction (Figure 4, Table 5).

The separation between these potentials is much larger for the neutral species **1** and **3** at about 1.6 V versus only about 1.0 V for $\mathbf{2}(PF_6)$ and $\mathbf{4}(PF_6)$. We attribute the wider stability range of **1** and **3** to the antiferromagnetic interaction between the metal and the radical anion ligand. Between corresponding complexes containing L_O and L_S ligands there is a distinct shift of about 0.3–0.4 V to more positive potentials for the sulfur system, reflecting the more facile reduction of thiocarbonyls versus carbonyl functions.[15] This observation also suggests mostly ligand-centered electron transfer in the redox series as summarized in Scheme 5.

The EPR silent compounds **1** and **3** can be oxidized and reduced electrolytically to EPR active species (Table 3). Figure 5 shows the observed spectra in frozen CH_2Cl_2/0.1 M Bu_4NPF_6 solution.

The anions could also be studied EPR spectroscopically at ambient temperature where they exhibit just one unresolved line. The data from Table 3 can be compared to a list[36a] of paramagnetic ruthenium complexes which ranges from almost pure Ru^{III} species (with large g anisotropy, $g_1 - g_3 > 0.5$) to radical complexes of diamagnetic Ru^{II} (with very small g anisotropy). The comparison suggests a predominantly ruthenium(III) situation for $\mathbf{1}^+$, according to the formulation $[(acac)_2Ru^{III}(L^0)]^+$. In contrast, the considerably but not completely diminished g anisotropy of the anions $\mathbf{1}^-$ and $\mathbf{3}^-$ suggests a mixed situation $[(acac)_2Ru^{III}(L^{2-})]^- \leftrightarrow [(acac)_2Ru^{II}(L^{\bullet-})]^-$ as has been similarly observed[37a] and discussed[37b] for oxidized and reduced $Ru(acac)_2$ complexes of deprotonated 2-aminophenol and 2-aminothiophenol.

UV–vis–NIR Spectroelectrochemical measurements using an OTTLE cell are illustrated by Figures 6–8 and summarized in Table 6.

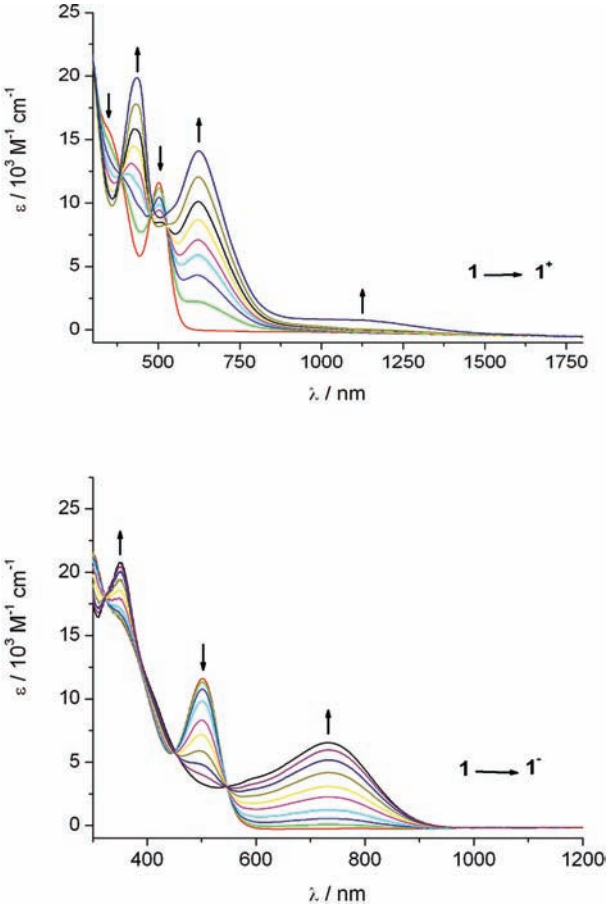

Figure 6. UV–vis–NIR Spectroelectrochemical response on reduction (top) and oxidation (bottom) of **1** in CH_2Cl_2/0.1 M Bu_4NPF_6.

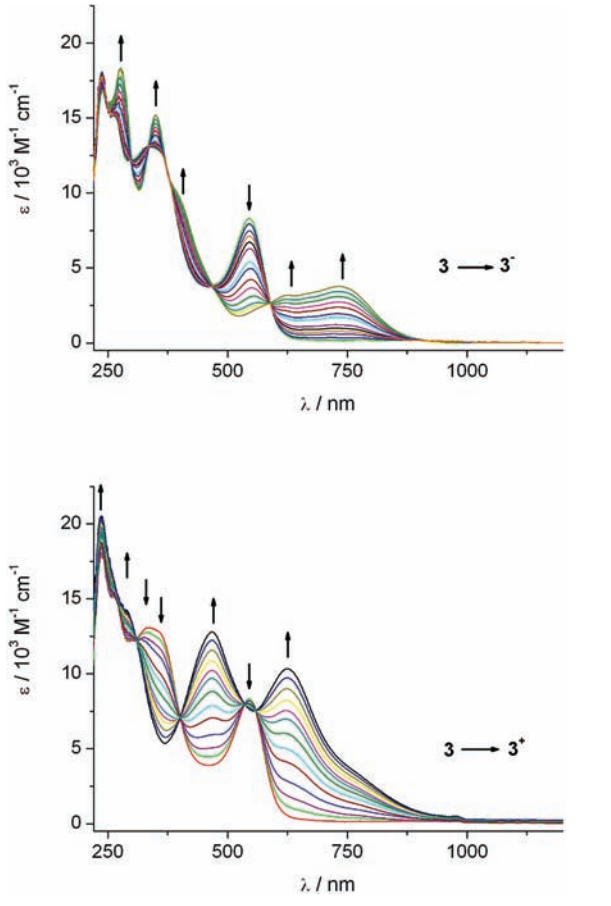

Figure 7. UV–vis–NIR Spectroelectrochemical response on reduction (top) and oxidation (bottom) of **3** in CH_2Cl_2/0.1 M Bu_4NPF_6.

On the basis of structural and EPR results and on TD-DFT calculations, the UV–vis–NIR spectroelectrochemical data are

dx.doi.org/10.1021/ic300439h | Inorg. Chem. 2012, 51, 6237–6244

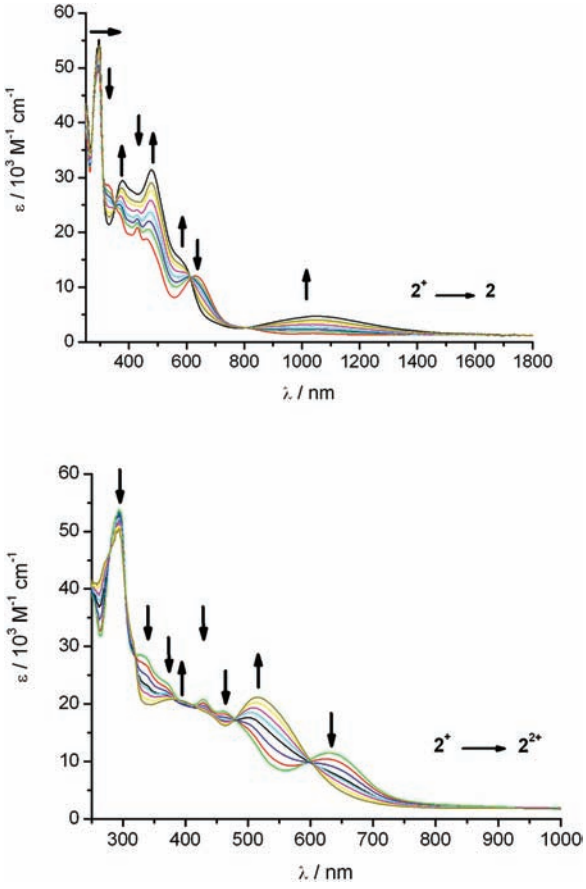

Figure 8. UV−vis−NIR Spectroelectrochemical response on oxidation (top) and reduction (bottom) of **2**(PF_6) in CH_2Cl_2/0.1 M Bu_4NPF_6.

Table 6. UV−vis−NIR Data for 1″−4″ from OTTLE Spectroelectrochemistry in CH_2Cl_2/0.1 M Bu_4NPF_6

compound	λ_{max} [nm] (ε [M^{-1} cm^{-1}])
1	349(16 000), 502(11 700)
$\mathbf{1}^+$	436(19 900), 625(14 100), 1100sh
$\mathbf{1}^-$	353(20 800), 733(6 500)
2	295(54 900), 378(29 500), 478(31 400), 577(15 500), 1039(4 800)
$\mathbf{2}^+$	295(53 500), 3334(28 400), 369(23 800), 429(20 800), 461(18 500), 630 (11500)
$\mathbf{2}^{2+}$	295(50 100), 381(21 000), 517(21 300)
3	335(13 100), 358(12 800), 545(8 300)
$\mathbf{3}^+$	285(14 400), 465(12 800), 625(10 400), 760sh
$\mathbf{3}^-$	276(18 400), 350(15 200), 400(9 700), 624(3200), 735(3 800)
4	291(48 100), 366(15 900), 420(13 800), 472(18 200), 560(6 600), 977(2 200)
$\mathbf{4}^+$	291(48 100), 339(14 200), 413(10 600), 438(10 500), 660(5 700)
$\mathbf{4}^{2+}$	262(27 200), 291(27 000), 316(23 300), 350(12 700), 539(12 500)

assigned as follows. The complexes **1** and **3** absorb in the visible because of the allowed HOMO-2−LUMO (Supporting Information, Figure S3) MLCT/IL transitions. On oxidation to the $Ru^{III}(L^0)$ form, new bands in the visible appear because of metal-to-ligand charge-transfer (MLCT) transitions. Reduction to a mixed $Ru^{III}(L^{2-})/Ru^{II}(L^{\bullet-})$ configuration according to EPR spectroscopy results in the emergence of band systems with maxima at about 735 nm, attributed to MLCT transitions.

Scheme 6

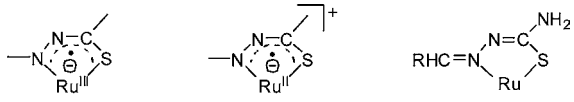

The cations $\mathbf{2}^+$ and $\mathbf{4}^+$ are radical anion complexes[38] with little metal participation at the SOMO. The long-wavelength absorption maxima are attributed to MLCT($L^{\bullet-}$) and MLCT-(bpy) transitions within the $[(bpy)_2Ru^{II}(L^{\bullet-})]^+$ configuration. On reduction to neutral $(bpy)_2Ru^{II}(L^{2-})$ there is a broad near-IR absorption, assigned to ligand-to-ligand charge transfer (LL′CT), with L^{2-} as donor and bpy as acceptor. Oxidation to the dications, tentatively associated with a $Ru^{III}(L^{\bullet-})$ configuration, produces absorption in the visible, attributed to MLCT/IL transitions. Remarkably, these values of about 500 nm for $\mathbf{2}^{2+}$ and $\mathbf{4}^{2+}$ coincide with those of **1** and **3** which confirms their structural identification as $Ru^{III}(L^{\bullet-})$ species.

CONCLUSION

The present study, employing two new redox-active hetero-1,3-diene ligands, shows that both L_O and L_S can behave as noninnocent ligands toward ruthenium complex fragments. According to crystal structure analysis, *all* four isolated forms (Scheme 4) contain the anion radical ligands,[38] $L_O^{\bullet-}$ or $L_S^{\bullet-}$. In connection with $[(bpy)_2Ru^{II}]^{2+}$ the ligands $L^{\bullet-}$ form stable radical complexes of a well established kind,[18b,37] but toward electron transfer generated $[(acac)_2Ru^{III}]^+$ they serve as components of antiferromagnetically coupled (S = 0) species $Ru^{III}(L^{\bullet-})$. The latter can be oxidized to EPR evidenced $Ru^{III}(L^0)$ compounds and reduced to anions with mixed $Ru^{III}(L^{2-})/Ru^{II}(L^{\bullet-})$ characteristics.

The rather different ancillary ligands, donating $acac^-$ and π accepting bpy, result in two related but separate redox series as illustrated in Scheme 5. In contrast, the L_O and L_S ligands do not cause a qualitatively different behavior of the complexes, the slight shifts of electrochemical potentials to higher values for the sulfur containing hybrid systems reflect the better π acceptor behavior of C═S vs C═O.[15]

The L_S containing radical complex alternatives as depicted in Scheme 6 invite a comparison with the formally similar NNCSRu five-membered chelate rings involving the popular thiosemicarbazone ligands.[39] These can bind ruthenium in various ways (see Scheme 6)[40] but never act as redox-active or radical ligands.[38]

ASSOCIATED CONTENT

Supporting Information

X-ray crystallographic files in CIF format for **1**, **2**(PF_6), **3**, **4**(PF_6), and **5**; Table S1 and Figure S1, illustrating the molecular structure of **5** from XRD analysis; Figures S2−S5 showing MO and spin density representations. This material is available free of charge via the Internet at http://pubs.acs.org.

AUTHOR INFORMATION

Corresponding Author

*E-mail: kaim@iac.uni-stuttgart.de.

Notes

The authors declare no competing financial interest.

dx.doi.org/10.1021/ic300439h | *Inorg. Chem.* 2012, 51, 6237−6244

■ ACKNOWLEDGMENTS

Financial support received from the Deutsche Forschungsgemeinschaft (Germany) is gratefully acknowledged. S.Z. thanks the Ministry of Education of the Czech Republic (Grant LD11086) for support.

■ REFERENCES

(1) (a) Kaim, W. *Inorg. Chem.* **2011**, *50*, 9752. (b) Kaim, W.; Schwederski, B. *Coord. Chem. Rev.* **2010**, *254*, 1580. (c) Kaim, W.; Olbrich-Deussner, B. In *Organometallic Radical Processes*; Trogler, W. C., Ed.; Elsevier: Amsterdam, The Netherlands, 1990; p 173. (d) Kaim, W. *Eur. J. Inorg. Chem.* **2012**, 343.

(2) (a) Jørgensen, C. K. *Coord. Chem. Rev.* **1966**, *1*, 164. (b) Ward, M. D.; McCleverty, J. A. *J. Chem. Soc., Dalton Trans.* **2002**, 275. (c) Chaudhuri, P.; Verdani, C. N.; Bill, E.; Bothe, E.; Weyhermüller, T.; Wieghardt, K. *J. Am. Chem. Soc.* **2001**, *123*, 2213. (d) Butin, K. P.; Beloglazkina, E. K.; Zyk, N. V. *Russ. Chem. Rev.* **2005**, *74*, 531. (e) Boyer, J. L.; Rochford, J.; Tsai, M.-K.; Muckerman, J. T.; Fujita, E. *Coord. Chem. Rev.* **2010**, *254*, 309.

(3) (a) Bhattacharya, S.; Gupta, P.; Basuli, F.; Pierpont, C. G. *Inorg. Chem.* **2002**, *41*, 5810. (b) Carugo, O.; Djinović, K.; Rizzi, M.; Bisi Castellani, C. *J. Chem. Soc., Dalton Trans.* **1991**, 1551.

(4) (a) Kaim, W.; Sieger, M.; Greulich, S.; Sarkar, B.; Fiedler, J.; Záliš, S. *J. Organomet. Chem.* **2010**, *695*, 1052. (b) Bock, H.; tom Dieck, H. *Angew. Chem.* **1966**, *78*, 549; *Angew. Chem., Int. Ed. Engl.* **1966**, *5*, 520. (c) van Koten, G.; Vrieze, K. *Adv. Organomet. Chem.* **1982**, *21*, 151. (d) Caulton, K. G. *Eur. J. Inorg. Chem.* **2012**, 435.

(5) Scarborough, C. C.; Wieghardt, K. *Inorg. Chem.* **2011**, *50*, 9773.

(6) (a) Ernst, S.; Kaim, W. *J. Am. Chem. Soc.* **1986**, *108*, 3578. (b) Kaim, W. *Coord. Chem. Rev.* **2002**, *230*, 127.

(7) Spikes, G. H.; Bill, E.; Weyhermüller, T.; Wieghardt, K. *Angew. Chem.* **2008**, *120*, 3015; *Angew. Chem., Int. Ed.* **2008**, *47*, 2973.

(8) (a) Balch, A. L. *J. Am. Chem. Soc.* **1973**, *95*, 2723. (b) Griffith, W. P. *Trans. Met. Chem.* **1993**, *18*, 250. (c) Pierpont, C. G.; Lange, C. W. *Prog. Inorg. Chem.* **1994**, *41*, 331.

(9) (a) Eisenberg, R.; Gray, H. B. *Inorg. Chem.* **2011**, *50*, 9741. (b) Vlcek, A. *Coord. Chem. Rev.* **2010**, *254*, 1357 , and following articles in that issue.

(10) (a) Maroney, M. J.; Trogler, W. C. *J. Am. Chem. Soc.* **1984**, *106*, 4144. (b) Gross, M. E.; Trogler, W. C.; Ibers, J. A. *J. Am. Chem. Soc.* **1981**, *103*, 192. (c) Gross, M. E.; Trogler, W. C.; Ibers, J. A. *Organometallics* **1982**, *1*, 732. (d) Overbosch, P.; van Koten, G.; Spek, A. L.; Roelofsen, G.; Duisenberg, A. J. M. *Inorg. Chem.* **1982**, *21*, 3908.

(11) (a) Poddel'sky, A. I.; Cherkasov, V. K.; Abakumov, G. A. *Coord. Chem. Rev.* **2009**, *253*, 291. (b) Lu, C. C.; Bill, E.; Weyhermüller, T.; Bothe, E.; Wieghardt, K. *Inorg. Chem.* **2007**, *46*, 7880. (c) Bessenbacher, C.; Kaim, W. *Z. Anorg. Allg. Chem.* **1989**, *577*, 39.

(12) Kaim, W. *Coord. Chem. Rev.* **2001**, *219*−*221*, 463.

(13) (a) Dürr, S.; Höhlein, U.; Schobert, R. *J. Organomet. Chem.* **1993**, *458*, 89. (b) Pilia, L.; Artizzu, F.; Espa, D.; Marchiò, L.; Mercuri, M. L.; Serpe, A.; Deplano, P. *Dalton Trans.* **2010**, *39*, 8139.

(14) Roy, S.; Sieger, M.; Sarkar, B.; Schwederski, B.; Lissner, F.; Schleid, Th.; Fiedler, J.; Kaim, W. *Angew. Chem.* **2008**, *120*, 6287; *Angew. Chem., Int. Ed.* **2008**, *47*, 6192.

(15) (a) Kar, S.; Sarkar, B.; Ghumaan, S.; Janardanan, D.; van Slageren, J.; Fiedler, J.; Puranik, V. G.; Sunoj, R. B.; Kaim, W.; Lahiri, G. K. *Chem.—Eur. J.* **2005**, *11*, 4901. (b) Patra, S.; Sarkar, B.; Maji, S.; Fiedler, J.; Urbanos, F. A.; Jimenez-Aparicio, R.; Kaim, W.; Lahiri, G. K. *Chem.—Eur. J.* **2006**, *12*, 489.

(16) Modelli, A.; Jones, D.; Rossini, S.; Distefano, G. *Tetrahedron* **1984**, *40*, 3257.

(17) (a) Barton, D. H. R.; Ducker, J. W.; Lord, W. A.; Magnus, P. D. *J. Chem. Soc., Perkin Trans. I* **1976**, 38. (b) Wolkoff, P.; Hammerum, S. *Can. J. Chem.* **1974**, *52*, 879.

(18) (a) Krejčik, M.; Danek, M.; Hartl, F. *J. Electroanal. Chem. Interfacial Electrochem.* **1991**, *317*, 179. (b) Kaim, W.; Ernst, S.; Kasack, V. *J. Am. Chem. Soc.* **1990**, *112*, 173.

(19) (a) Kasahara, Y.; Hoshino, Y.; Shimizu, K.; Sato, G. P. *Chem. Lett.* **1990**, 381. (b) Sullivan, B. P.; Salmon, D. J.; Meyer, T. J. *Inorg. Chem.* **1978**, *17*, 3334.

(20) Starr, J. T.; Rai, G. S.; Dang, H.; McNelis, B. J. *Synth. Commun.* **1997**, *27*, 3197.

(21) Bock, H.; Baltin, E.; Kroner, J. *Chem. Ber.* **1966**, *99*, 3337.

(22) (a) Sheldrick, G. M. *Acta Crystallogr.* **2008**, *A64*, 112. (b) Spek, A. L. *Acta Crystallogr.* **2009**, *D65*, 148.

(23) Frisch, M. J.; Trucks, G. W.; Schlegel, H. B.; Scuseria, G. E.; Robb, M. A.; Cheeseman, J. R.; Scalmani, G.; Barone, V.; Mennucci, B.; Petersson, G. A.; Nakatsuji, H.; Caricato, M.; Li, X.; Hratchian, H. P.; Izmaylov, A. F.; Bloino, J.; Zheng, G.; Sonnenberg, J. L.; Hada, M.; Ehara, M.; Toyota, K.; Fukuda, R.; Hasegawa, J.; Ishida, M.; Nakajima, T.; Honda, Y.; Kitao, O.; Nakai, H.; Vreven, T.; Montgomery, Jr., J. A.; Peralta, J. E.; Ogliaro, F.; Bearpark, M.; Heyd, J. J.; Brothers, E.; Kudin, K. N.; Staroverov, V. N.; Kobayashi, R.; Normand, J.; Raghavachari, K.; Rendell, A.; Burant, J. C.; Iyengar, S. S.; Tomasi, J.; Cossi, M.; Rega, N.; Millam, J. M.; Klene, M.; Knox, J. E.; Cross, J. B.; Bakken, V.; Adamo, C.; Jaramillo, J.; Gomperts, R.; Stratmann, R. E.; Yazyev, O.; Austin, A. J.; Cammi, R.; Pomelli, C.; Ochterski, J. W.; Martin, R. L.; Morokuma, K.; Zakrzewski, V. G.; Voth, G. A.; Salvador, P.; Dannenberg, J. J.; Dapprich, S.; Daniels, A. D.; Farkas, Ö.; Foresman, J. B.; Ortiz, J. V.; Cioslowski, J.; Fox, D. J. *Gaussian 09*, Revision B.01; Gaussian, Inc.: Wallingford, CT, 2009.

(24) te Velde, G.; Bickelhaupt, F. M.; van Gisbergen, S. J. A.; Fonseca Guerra, C.; Baerends, E. J.; Snijders, J. G.; Ziegler, T. *J. Comput. Chem.* **2001**, *22*, 931.

(25) *ADF 2010.01*; SCM, Vrije Universiteit: Amsterdam, The Netherlands; http://www.scm.com.

(26) Hariharan, P. H.; Pople, J. A. *Theor. Chim. Acta* **1973**, *28*, 213.

(27) Andrae, D.; Haeussermann, U.; Dolg, M.; Stoll, H.; Preuss, H. *Theor. Chim. Acta* **1990**, *77*, 123.

(28) Perdew, J. P.; Burke, K.; Ernzerhof, M. *Phys. Rev. Lett.* **1996**, *77*, 3865.

(29) Adamo, C.; Barone, V. *J. Chem. Phys.* **1999**, *110*, 6158.

(30) Cossi, M.; Rega, N.; Scalmani, G.; Barone, V. *J. Comput. Chem.* **2003**, *24*, 669.

(31) Becke, A. D. *J. Chem. Phys.* **1993**, *98*, 5648.

(32) (a) Becke, A. D. *Phys. Rev. A* **1988**, *38*, 3098. (b) Perdew, J. P.; Wang, Y. *Phys. Rev. B* **1992**, *45*, 13244. (c) Perdew, J. P. *Phys. Rev. B* **1986**, *33*, 8822.

(33) (a) van Lenthe, E.; van der Avoird, A.; Wormer, P. E. S. *J. Chem. Phys.* **1998**, *108*, 4783. (b) van Lenthe, E.; van der Avoird, A.; Wormer, P. E. S. *J. Chem. Phys.* **1997**, *107*, 2488.

(34) (a) Sarkar, B.; Patra, S.; Fiedler, J.; Sunoj, R. B.; Janardanan, D.; Lahiri, G. K.; W. Kaim, W. *J. Am. Chem. Soc.* **2008**, *130*, 3532. (b) Doslik, N.; N.; Sixt., T.; W. Kaim, W. *Angew. Chem.* **1998**, *110*, 2521; *Angew. Chem., Int. Ed.* **1998**, *37*, 2403.

(35) Li, W.-K.; Zhou, G.-D.; Mak, T. C. W. *Advanced Structural Inorganic Chemistry*; Oxford University Press: Oxford, U.K., 2008; p 522.

(36) (a) Chen, H.; Ikeda-Saito, M.; Shaik, S. *J. Am. Chem. Soc.* **2008**, *130*, 14778. (b) Kaim, W.; Schwederski, B. *Coord. Chem. Rev.* **2010**, *254*, 1580.

(37) (a) Patra, S.; Sarkar, B.; Mobin, S. M.; Kaim, W.; Lahiri, G. K. *Inorg. Chem.* **2003**, *42*, 6469. (b) Waldhör, E.; Schwederski, B.; Kaim, W. *J. Chem. Soc., Perkin Trans. 2* **1993**, 2109.

(38) Kaim, W. *Coord. Chem. Rev.* **1987**, *76*, 187.

(39) Lobana, T. S.; Sharma, R.; Bawa, G.; Khanna, S. *Coord. Chem. Rev.* **2009**, *253*, 977.

(40) Datta, S.; Drew, M. G. B.; Bhattacharya, S. *Indian J. Chem.* **2011**, *50A*, 1403.